Volume-3, Issue-7, July-2014 • ISSN No 2277 - 8160

Research Paper Chemistry

Synthesis and Characterisation of Citric Acid Based Polyester - Hydroxyapatite Nanocomposites

Indira R.	PG and Research Department of Chemistry, Presidency College, Chennai – 600 005, India.
Sivakumar E. K .T.	Centre for Nanoscience and Technology, Anna University, Chennai 600 025, India.
Hariharapriya G.	PG and Research Department of Chemistry, Presidency College, Chennai – 600 005, India.
Jaisankar V.	PG and Research Department of Chemistry, Presidency College, Chennai – 600 005, India.

ABSTRACT

The incorporation of nanoscale hydroxyapatite (n-HAp) into biodegradable polymers can potentially mimic the native structure of bone and influence the mechanical properties and the extent of bioactivity. In this investigation, nanocomposites of poly(1,6-Hexanediol-Maleate-Citrate) (PHMC) containing 5, 10 and 15 wt% n-HAp were fabricated and characterised. The polyester was characterized by solubility studies, 1H NMR and 13C NMR spectral studies. Fourier transform infrared (FT-IR) spectroscopy was performed to analyze the interactions between n-HAp and PHMC matrix. X-ray diffraction analysis was carried out to study the structural information of nanocomposite. Tensile tests were conducted to evaluate the mechanical properties of the nanocomposites and differential scanning calorimetry (DSC) was carried out to study the thermal properties of n-HAp/PHMC nanocomposites. The Young's modulus and tensile strength of nanocomposites were increased with higher concentration of n-HAp. Thermal studies showed that the Tg of the nanocomposites decreased with increase in n-HAp contents. The morphological studies were characterized by SEM. This study provides an insight into how the hydroxyapatite nanoparticle content can modulate the physical properties of n-HAp/PHMC nanocomposites.

KEYWORDS : Nanohydroxyapatite, Sol-gel method, Thermal studies, Nanocomposites

1. INTRODUCTION

In the recent past, the synthesis of new biodegradable polymeric nanocomposite has attracted significant interest to fulfill the unmet needs of healthcare. Biodegradable aliphatic polyester elastomers have been recognized as one of the most promising biodegradable materials because they are easily susceptible to biological attack and their degradation products are non-toxic and can enter the metabolic cycles of bio-organisms [1,2]. Tissue engineering, which applies methods from engineering and life sciences to create artificial constructs to direct tissue regeneration, has attracted many scientists and surgeons with a hope to treat patients in a minimally invasive and less painful way [3].The use of mesenchymal stem cells has been increasingly popular for the treatment of bone defects. These cells can be easily expanded to high cell numbers and the addition of mesenchymal cells facilitates the healing of bone defects. However, mesenchymal stem cells suspensions are difficult to maintain within a bone defect and do not provide any biomechanical stability. Hence, mesenchymal stem cells are combined with scaffolds for tissue engineering applications.

The standard biomaterials used for scaffolds is the polyester poly(L-lactide)(PLLA). The disadvantage of using PLLA is that it undergoes slow and bulk degradation which results in chronic inflammation, fracture, pain and revision surgeries. In order to increase the osteoconductive and osteogenic properties, an apatite material such as hydroxyapatite (HAp) is incorporated into biomaterials. Calcium phosphate ceramics such as hydroxyapatite (HAp) are often considered for these applications because HA makes up the inorganic phase of native bone and is biocompatible, osteoconductive, and osteoinductive [4-7]. For these reasons calcium phosphate ceramics have gained acceptance in both dental and orthopedic applications, including the repair of bone defects, augmentation of the alveolar ridge, tooth root replacement, ear implants, spine fusion, and bone cements [8-12]. However, the main limitation of HAp is the formation of microcracks induced during harsh processing conditions and its brittleness [13-15]. Furthermore, processing under high temperatures can cause changes in crystallinity and Ca/P stoichiometry [16]. To overcome these disadvantages, hydroxy apatite was combined with biodegradable polyesters [17-22].

Herein, we report on the synthesis and characterization of new biocompatible and biodegradable elastomer, poly(1,6-Hexanediol-maleate-citrate). The incorporation of nanohydroxyapatite (n-HAp) into the elastomer is expected to increase the mechanical properties of the nanocomposites. Tensile and thermal properties of the nanocomposites were evaluated. The morphology of the nanocomposites was studied.

2. Experimental

2.1. Materials

Maleic acid (MA) (99%) (MERCK AR grade), hexanediol (HD) (99%) (Lancaster AR grade) and citric acid (CA) were obtained and used without further purification. Nano-hydroxyapatite (n-HAp) was synthesized by sol-gel method [23]. The other materials and solvents used for the analytical methods were of analytical grade.

2.2. Synthesis of nano-hydroxyapatite

0.25M Phosphoric acid (PA) solution was prepared and to this solution ammonia (MERCK AR grade) was added in drops and stirred till a constant pH = 10. 1M Calcium nitrate tetrahydrate (CNT, Aldrich) solution was prepared and was slowly added to the PA-NH_3 solution, maintaining a Ca/P ratio of 1.67. Further small amounts of ammonia was added to the solution to maintain a constant pH=10. The solution was vigorously stirred for 1hr and kept for ageing for 24 hr at room temperature. The gel obtained after ageing was dried at 65°C for 24 hrs in a dry oven. The powders obtained from dried gel were washed repeatedly using double distilled water to remove NH_4^+ and NO_3^-. After washing, the powder was calcined in air at 500°C for 30 min in an electric furnace.

2.3. Preparation of n-HAp/poly((hexanediol-maleate-citrate) (PHMC) nanocomposites

Equimolar amounts of both HD and acids [HD:(CA + MA) = 1:1] were added to a round bottomed flask and melted together at 160-165°C followed by mixing at 140-145°C for 1hr under constant steam of nitrogen to obtain PHMC pre-polymer. The pre-polymer was then mixed to incorporate 5%, 10% and 15% by weight n-HAp. PHMC pre-polymer dissolved in ethanol (1:1 w/v) was mixed with the desired amount of n-HAp powder. The PHMC-n-HAp mixture was stirred

to get homogeneous solution and cast into Teflon dishes and left in an oven at 110ºC for 2 days for post-curing. The nanocomposites with 0, 5, 10 and 15 wt% of n-HAp were named as P0, P5, P10, and P15 respectively.

2.4. Characterisation

2.4.1. Solubility

The solubility of the synthesized polyester, PHMC, was determined in various solvents qualitatively.

2.4.2. ^{1}H NMR measurements

^{1}H NMR spectra of the synthesized copolyester were recorded on AV 3500 MHz Spectrometer by using 7% wt of trifluoroacetic acid/$CDCl_3$ mixed solvent.

2.4.3. ^{13}C NMR measurements

^{13}C NMR spectra of the synthesized copolyester were recorded using deuterated chloroform as solvent at 300-600 MHz.

2.4.4. Fourier- Transform Infrared (FTIR) spectroscopy

IR spectra of the n-HAp, copolyester and nanocomposite were recorded using a perkin Elmer IR spectrometer in the range of 700 cm^{-1} to 4500 cm^{-1}. The samples were embedded in KBr pellets.

2.4.5. X-Ray Diffraction (XRD) analysis

A Siemens D 500 diffractometer with CuKα filtered radiations was used for assessing the crystallinity of n-HAp, copolyester and nanocomposite. The samples were scanned over the 2θ range from 5º to 80º.

2.4.6. Differential Scanning Calorimetry (DSC)

The DSC scans of the copolyester and the nanocomposite were recorded at a heating rate of 10ºC/min using a Perkin-Elmer Pyris I analyser. Indium was used as the calibration standard.

2.4.7. Mechanical properties

The mechanical properties of the films of copolyester and nanocomposites were measured using tensitometer (model:K10KS-0128) equipped with 100N load cell at room temperature. The film samples were prepared according to the ASTM standard D 882-01 were tested at a rate of 10mm/min. Tensile strength and young's modulus were calculated from the stress-strain curve. [24]

2.4.8. Scanning Electron Microscopy (SEM)

The structure and morphology of the n-HAp powder, polyester and nanocomposite thin films were studied using a HITACHI S-3000 scanning electron microscope (SEM).

2.4.9. Transmission Electron Microscopy (TEM)

Transmission electron microscope (TEM) (HR-TEM, Model-HITACHI, H-7650) was used to observe the morphology and the particle size of calcined n-HAp powders.

3. Results and Discussion

3.1. Solubility studies

The solubility of the synthesised random copolyester was tested qualitatively in various organic solvents and the results are presented in Table 1.

Table 1 Solubility of copolyester PHMC

Polymer	Acetone	$CHCl_3$	DMSO	Methanol	Ethanol	THF	DMF	Water
PHMC	+ + +	+ + +	+ + +	+ + +	+ + +	+ +	+ +	− − −

+++ - Freely Soluble, ++ - Soluble, −−− - Insoluble

The synthesised copolyester is freely soluble in acetone, $CHCl_3$, DMSO, methanol and ethanol. The polyester is soluble in THF and DMF and insoluble in water.

3.2. ^{1}H NMR spectra of polyester

The structure of the repeating units present in the copolyester can be analysed qualitatively and quantitatively by ^{1}H NMR spectroscopy. Figure 1 shows the ^{1}H NMR spectra of synthesized copolyester PHMC. ^{1}H-NMR spectra of the sample show the expected characteristic peaks.

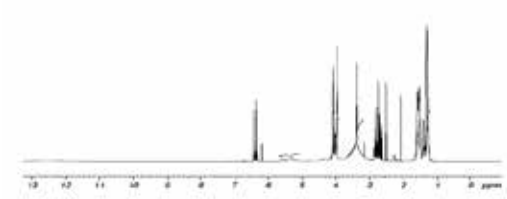


Fig. 1 ^{1}H NMR spectra of copolyester PHMC

The chemical shift values obtained from 1H NMR spectra of copolyester are as follows. The peak observed at 2.8-2.6 ppm, was assigned to –CH2– from citric acid. The peak located at 3.36 ppm correspond to central methylene protons of 1,6-hexanediol. The peaks observed between 6 and 7 ppm were assigned to the protons of –CH=CH– from maleic acid incorporated into the polymer chain.

3.3. ^{13}C NMR spectra of polyester

The chemical shift values of carbons present in different environments of the synthesised copolyester can be analysed by ^{13}C NMR spectroscopy. Figure 2 shows the ^{13}C NMR spectra of synthesized copolyester PHMC.

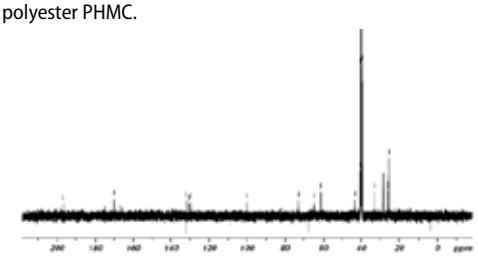
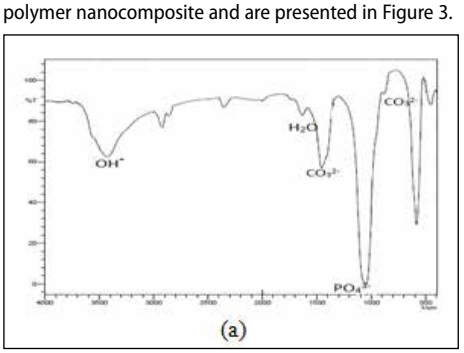


Fig. 2 ^{13}C NMR spectra of copolyester PHMC

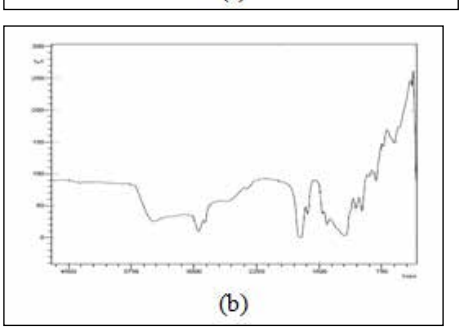
The chemical shift values obtained from ^{13}C NMR spectra of copolyester are as follows. The peaks located at 28–29 and 23–26 ppm, were assigned to $–CH_2–$ from diacids. The peak located at 169.83 ppm was assigned to carbonyl carbon atom of the ester group and peaks located at 65–61 ppm were assigned to $–CH_2$-CO– group. The peak at 130.51 ppm was assigned to -CH=CH- from maleic acid and the peak at 40.44 ppm was assigned to $–CH_2–$ from citric acid.

3.4. Fourier-Transform Infrared (FT-IR) spectroscopy

FT-IR spectra have been recorded for n-HAp, random copolyester and polymer nanocomposite and are presented in Figure 3.



(a)



(b)

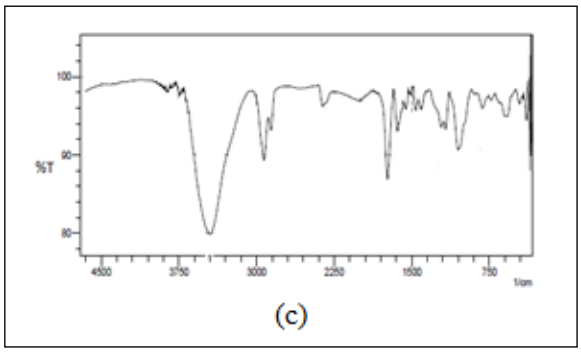
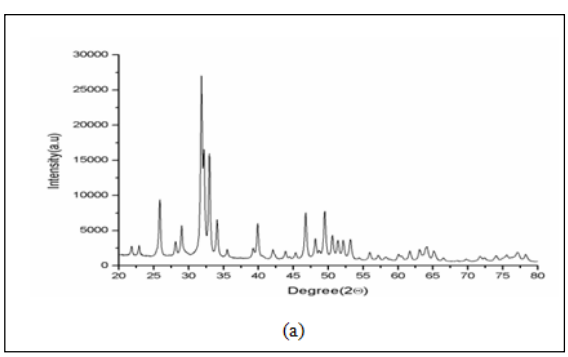


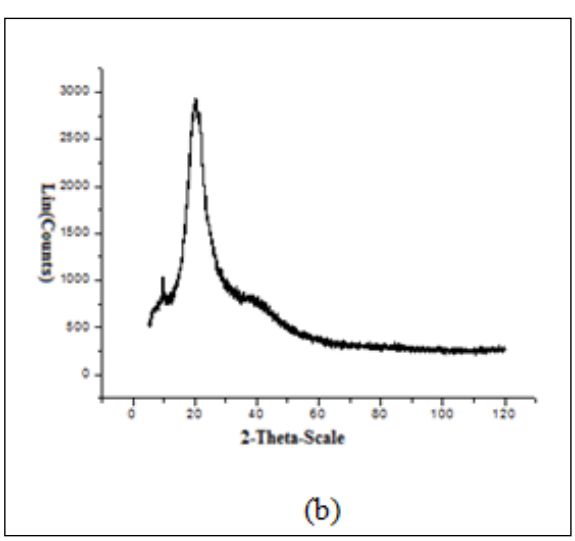
Fig. 3 FT-IR spectra of (a) n-HAp, (b) copolyester PHMC and (c) 15% n-HAp/PHMC nanocomposite

In spectra (a) a strong band of PO43- group was seen at 1042 cm-1 and 1050 cm-1 due to symmetric stretching vibration. The spectra possessed a broad band ranging between 3350 cm-1 and 3550 cm-1 shows the presence of –OH group. H2O band was also observed at 1632 cm-1. In spectra (b) the pronounced peaks at 1690–1750 cm−1 suggest the presence of carbonyl (C=O) groups from the ester bond and pendent carboxylic acid from the citric acid [25]. The shoulder peak of a lower wavelength at 1639 cm−1 proves the presence of the olefin moiety [26] from maleic acid. The bands centered at around 2944 cm−1 were assigned to methylene (-CH2-) groups for diacids/diols. Hydrogen-bonded hydroxyl functional groups showed absorbance as a broad peak centered at 3570 cm−1. It seems that the spectra of (c) were the superimposing of n-HAp on spectra (b) and no new peaks appeared in the spectra of the nanocomposite.

3.5. XRD analysis

The XRD patterns of n-HAp, copolyester and polymer nanocomposite are shown in Figure 4.





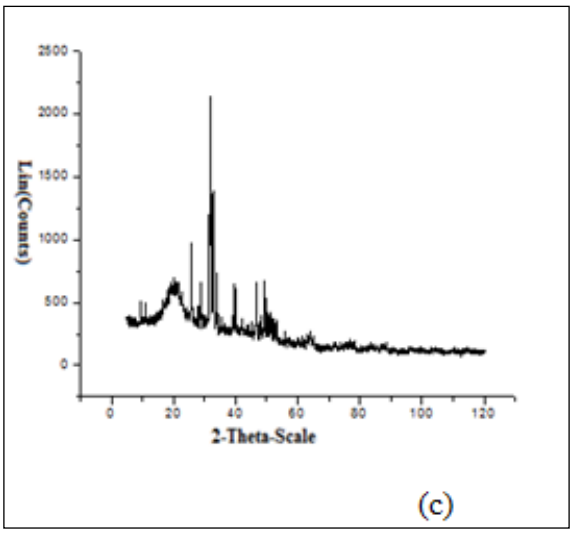


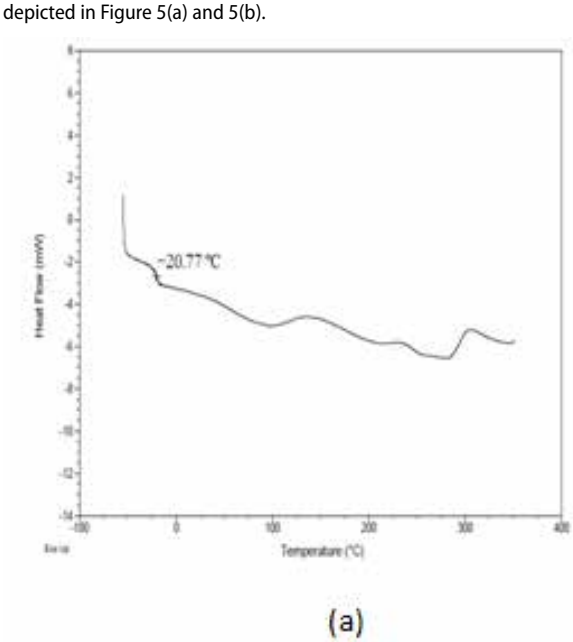
Fig. 4 X-ray diffraction pattern of (a) n-HAp, (b) copolyester PHMC and (c) 15% n-HAp/PHMC nanocomposite

XRD pattern of the dried HAp gel powder calcined at temperature 500°C showed mainly broad peaks of HAp and no characteristic peaks of impurities were observed, indicating that the product was of high purity. The amorphous HAp powders that were obtained at lower temperatures in this study are expected to be more metabolically active than the fully developed crystalline hydroxyapatite structure.

XRD pattern of amorphous polymers shows less sharp and highly intense peaks whereas the nanocomposites of crystalline polymer show sharper and highly intensed peaks. This is due to the development of crystallinity in nanocomposites. Highly intense peaks occur in the pattern of nanocomposite due to the presence of inserted n-HAp powder in the polymer matrix.

3.6. Thermal analysis

The thermal properties of polyesters and polymer nanocomposites were studied from Differential Scanning Calorimetry, DSC analysis. The DSC heating thermograms of PHMC and 15% of n-HAp/PHMC are depicted in Figure 5(a) and 5(b).



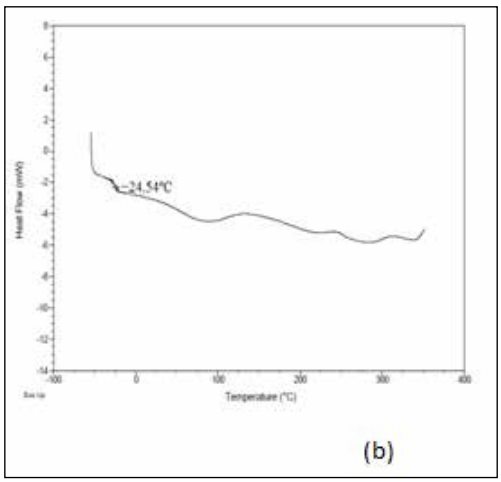


Fig. 5 DSC thermogram of (a) PHMC and (b) 15% n-HAp/ PHMC nanocomposite

It can be seen that all of the nanocomposites were amorphous, and no crystallization melting peaks were found. The glass transition temperature (Tg) of PHMC matrix is around −20.77°C. When n-HAp was incorporated, the Tg of the the nanocomposite is affected by chemical cross linking density, resulted in the decreased glass transition temperature of −24.54°C.

3.7. Mechanical properties

The mechanical properties of the synthesized copolyester and nanocomposite are tabulated in Table 2.

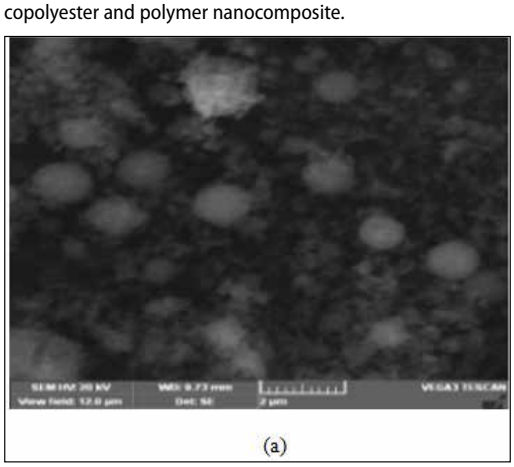
%n-HAp	Tensile Strength (MPa)	Young's Modulus (MPa)	Elongation at Break (%)
0	0.037	0.19	21.06
5	0.060	0.234	37.20
10	0.067	0.48	21.29
15	0.075	0.81	13.95

Table 2 Mechanical properties of nanocomposites

As shown in Table 2, it can be seen obviously that with increasing n-HAp content from 0 wt% to 15 wt% in the nanocomposite, the tensile strength and the modulus of nanocomposites prominently increased, meanwhile, the elongation at break of the nanocomposites reduced. The tensile strength and the modulus of the virgin PMHC elastomer are relatively lower than their nanocomposites because the molecular chains could be cleaved by high-shearing force, so the cross-link density of PMHC decreased here.

3.8. Scanning Electron Microscopy (SEM) analysis

The morphologies of n-HAp, polyester and nanocomposite were examined by SEM analysis. Figure 6 shows the SEM images of n-HAp, copolyester and polymer nanocomposite.



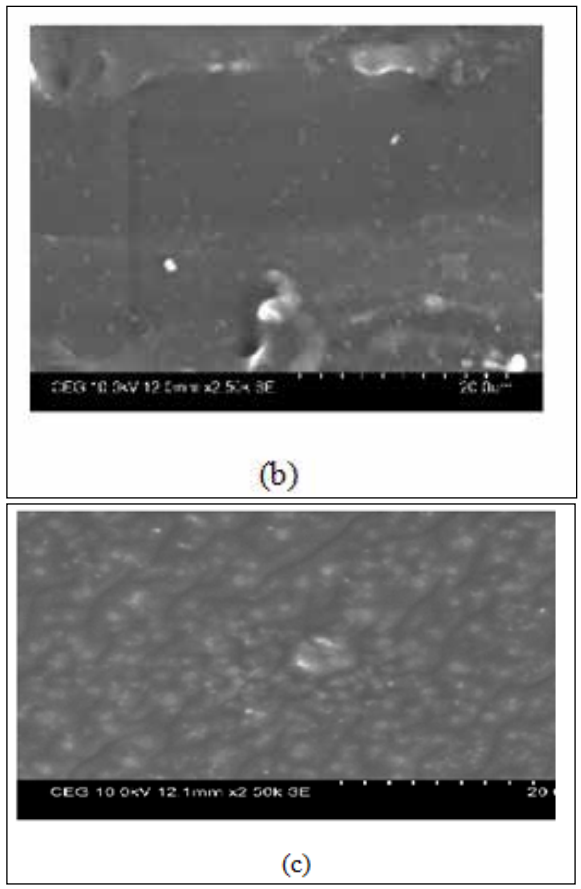
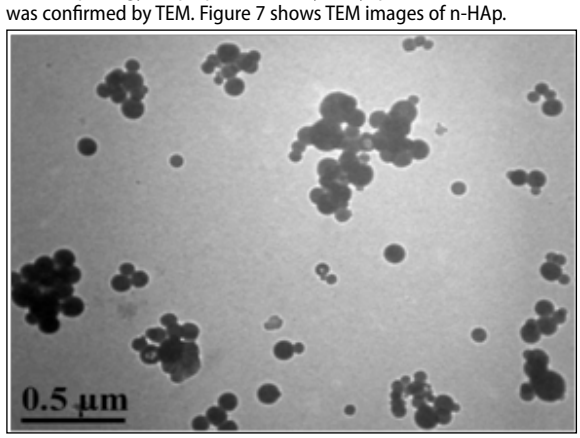


Fig. 6 SEM image of (a) n-HAp, (b) copolyester PHMC and (c) 15% n-HAp/PHMC nanocomposite

Figure 6(a) shows the SEM image of HAp calcined at 500°C. The powder appears to be of crushed angular shape which was taken at higher magnification reveals single particle of HAp is made up of agglomeration of nano sized grains. The nucleation and growth of HAp can be described by nucleation-aggregation-agglomeration theory [27] explained by Rodriguez et al. The grains formed may be agglomerated due to the formation of the gel during the synthesis. Figure 6(b) shows the SEM image of polyester film. The distribution of n-HAp particles in polymers was shown in Figure 6(c) depicted that there were no clear agglomeration can be found in the composites and relatively strong interfacial interaction between n-HAp and polymer matrix for the polymers filled with 15 wt% n-HAp.

3.9. Transmission Electron Microscopy (TEM)

The morphology of prepared nanohydroxyapatite sintered at 500°C was confirmed by TEM. Figure 7 shows TEM images of n-HAp.



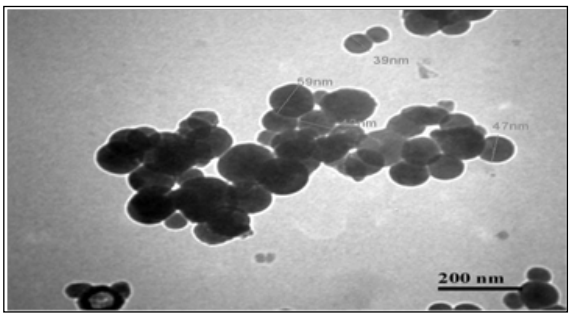


Fig. 7 TEM images of n-HAp

The TEM images of n-HAp powders fabricated by sol-gel method were in the sub-micron to nano-size range with all having dimensions of 30–70 nm.

4. Conclusions

In this study, a new type of copolyester has been synthesised by a simple catalyst-free melt polycondensation method with 1,6-hexane diol, citric acid and maleic acid as starting monomers. The nanostructured hydroxyapatite powder via sol-gel method using calcium and phosphorous precursors and the n-HAp/polyester nanocomposite were prepared. The chemical, physical and physico-chemical characteristics such as chemical structure, strength, elasticity and morphology were studied using spectral, thermal and mechanical methods. The materials were elastomeric in nature which is evident from thermal and mechanical analysis. The mechanical properties of PHMC elastomer is improved by incorporating n-HAp due to strong interfacial interaction and relatively uniform distribution of n-HAp. The PHMC and n-HAP/PHMC nanocomposite had appreciable mechanical and thermal properties which substantiate their cross-linking abilities. The developed new material will significantly improve the ease of fabrication and performance of biocompatible elastomers for future tissue engineering applications.

REFERENCES

[1] Rizzarelli, P., Impallomeni, G., Montaudo, G. (2004). Biomacromolecules, 5, 433–444. | [2] Lindstro¨m, A., Albertsson, A-C., Hakkarainen, M., (2004). Polym Degrad Stab, 83, 487–493. | [3] Seol, Y. J., Lee, J. Y., Park, Y. J., Lee, Y. M., Ku, Y., Rhyu, I. C., Lee, S. J., Han, S. B., Chung, C. P. (2004). Biotechnology Letters, 26, 1037-1041. | [4] Giannoudis, P.V., Dinopoulos, H., Tsiridis, E. (2005). Injury, 36, S20–27. | [5] LeGeros, R.Z. (2002). Clin Orthop Relat Res, 395, 81–98. | [6] Hing, K.A. (2005). Int J Appl Ceram Technol, 2, 184–199. | [7] Ruhé, P.Q., Kroese-Deutman, H.C., Wolke, J.G.C., Spauwen, P.H.M., Jansen, J.A. (2004). Biomaterials, 25, 2123–2132. | [8] Larsson, S., Bauer, T.W. (2002). Clin Orthop Relat Res, 395, 23–32. | [9] Driessens, F., Verbeeck, R. (1985). Calcif Tissue Int, 37, 376–380. | [10] Valentini, P., Abensur, D., Wenz, B., Peetz, M., Schenk, R. (2000). Int J Periodontics Restorative Dent, 20, 245–253. | [11] Wagner, J.R. (1989). J Oral Implantol, 15, 186–192. | [12] Katti, K.S. (2004). Colloids Surf B Biointerfaces, 39, 133–142. | [13] Cooke, F.W. (1992). Clin Orthop Relat Res, 276, 135–146. | [14] Kundu, B., Sinha, M.K., Mitra, S., Basu, D. (2005). Indian J Ophthalmol, 53, 235–241. | [15] de Groot, K. (1993). Ceram Int, 19, 363–366. | [16] Landi, E., Tampieri, A., Celotti, G., Vichi, L., Sandri, M. (2004). Biomaterials, 25, 1763–1770. | [17] Causa, F. et al. (2006). J Biomed Mater Res A, 76, 151–162. | [18] Ignatius, A.A., Betz, O., Augat, P., Claes, L.E. (2001). J Biomed Mater Res, 58, 701–709. | [19] Rizzi, S.C., Heath, D.J., Coombes, A.G., Bock, N., Textor, M., Downes, S. (2001). J Biomed Mater Res, 55, 475–486. | [20] Furukawa, T., Matsusue, Y., Yasunaga, T., Nakagawa, Y., Okada, Y., Shikinami, Y., et al. (2000). J Biomed Mater Res, 50, 410–419. | [21] Scaglione, S., Lazzarini, E., Ilengo, C., Quarto, R. (2010). J Tissue Eng Regen Med, 4, 505–513. | [22] Wagoner Johnson, A.J., Herschler, B.A. (2011). Acta Biomater, 7, 16–30. | [23]Sanosh, K. P., Min-cheol chu, Balakrishnan, A., Kim, T. and seong-jai cho. (2009). Bull Mater Sci, 32, 465–470. | [24]Yang, J., Webb, A.R., Pickerill, S.J., Hageman, G., Ameer, G.A. (2006). Biomaterials, 27, 1889. | [25] Kaihara, S., Matsumura, S., Fisher, J.P. (2008). Eur J Pharm Biopharm, 68, 67. | [26]Behravesh, E., Shung, A.K., Jo. S., Mikos, A.G. (2002). Biomacromolecules, 3,153. | [27]Rodríguez-Clemente, R., López-Macipe, A., Gómez-Morales, J., Torrent-Burgués, J. and Castãno, V. M. (1998). J. Eur Ceram Soc, 18, 1351. |